Available online at www.sciencedirect.com
ScienceDirect
Catalysis Today 121 (2007) 27–38
CATALYSIS TODAY
www.elsevier.com/locate/cattod

Selective hydrogenation of unsaturated nitriles to unsaturated amines over amorphous CoB and NiB alloys doped with chromium

Pavel Kukula [a,*], Vendula Gabova [a], Klara Koprivova [b], Pavel Trtik [c]

[a] *Institute for Chemical and Bioengineering, ETH Zurich, 8092 Zurich, Switzerland*
[b] *Institute of Chemical Technology, Technicka 5, 166 28 Prague 6, Czech Republic*
[c] *Institute for Mechanical Systems, ETH Zurich, 8092 Zurich, Switzerland*

Available online 21 December 2006

Abstract

Amorphous binary (CoB, NiB) and ternary (CoBCr, NiBCr) alloys prepared by chemical reduction with $NaBH_4$ were characterized by atomic absorption spectroscopy (AAS), nitrogen physisorption (BET), X-ray diffraction (XRD), temperature programmed desorption (TPD), temperature programmed reduction (TPR), hydrogen chemisorption, scanning electron microscopy (SEM) coupled with energy dispersive X-ray analysis (EDX) and X-ray photoelectron spectroscopy (XPS) and the influence of their properties on catalytic performance in the hydrogenation of unsaturated nitriles to unsaturated amines was studied. The hydrogenation over NiB(Cr) catalysts lead to preferential hydrogenation of the C=C bond, whereas the hydrogenation over CoB(Cr) catalysts occurred preferentially to the unsaturated amine. Addition of chromium dramatically increased the activity of both NiB and CoB catalysts, due to its effect on the binding energy of adsorbed hydrogen and the adsorption strength of the nitrile functional group. Amorphous cobalt borides treated with sodium hydroxide can hydrogenate unsaturated nitriles to primary unsaturated amines with medium-to-high selectivity without the presence of ammonia.

Keywords: Chemoselective hydrogenation; Unsaturated nitriles; Unsaturated amines; CoB; NiB; Cr-doped amorphous alloy

1. Introduction

Nitrile hydrogenation is an important process for the production of various amines, which are widely used as intermediates in many branches of chemical industry. The most frequently applied process for the production of amines is the heterogeneous catalytic hydrogenation [1]. A broad range of commercially available nitriles makes this process even more important. In many cases, however, the molecules to be hydrogenated contain several reducible groups and only the desired one has to be reduced. The selective hydrogenation of unsaturated nitriles to the corresponding unsaturated amines is of interest, because unsaturated amines are valuable intermediates in the pharmaceutical, agrochemical and specialty and fine chemicals industry [2–5]. To tune the selectivity towards the unsaturated amine is a considerable challenge, because the hydrogenation of the C=C bond and the formation of a saturated nitrile, and consequently saturated amine, is thermodynamically more favourable.

The reactivity of the C=C bond towards hydrogenation decreases when it is sterically hindered or far away from the nitrile group [6–9]. Molecules with C=C and C≡N groups in conjugation or in close proximity are much more difficult to reduce selectively [9–12]. Nevertheless, it has been shown recently that with the proper catalytic system, a relatively high selectivity to unsaturated amine can be obtained [9,13]. Several factors play a crucial role in the selectivity: the type of catalyst, the catalyst promoters, the presence of ammonia and the type of solvent. Previous studies demonstrated the suitability of Raney-type catalysts in the chemoselective hydrogenation of unsaturated nitriles [9,13]. Under optimized conditions, a selectivity of up to 80% to 3-phenyl-allylamine at a conversion above 90% was obtained during the hydrogenation of cinnamonitrile with a Cr-doped Raney cobalt in methanol saturated with ammonia. The presence of ammonia was essential not only to suppress the formation of unwanted secondary amines, but also to enhance the selectivity to unsaturated amine. Replacing ammonia by sodium or lithium

* Corresponding author.
E-mail address: pavel.kukula@chem.ethz.ch (P. Kukula).

0920-5861/$ – see front matter © 2006 Elsevier B.V. All rights reserved.
doi:10.1016/j.cattod.2006.11.009

hydroxides led to more active, but significantly less selective catalysts [13]. To omit the ammonia in this reaction without a significant loss in the selectivity, a new type of catalyst has to be developed.

Amorphous metal alloys prepared by reduction of the metal salt with various borohydrides are well-known catalysts since the 1980s [14–18]. They are comparable in activity to Raney catalysts, but show better selectivity in many hydrogenation reactions [18]. The unique structure and high concentration of coordinatively unsaturated sites of amorphous metal alloys result in higher activity and selectivity then obtained with their crystalline counterparts [16,17]. The simple preparation and easy modification by additives makes the metal alloy catalysts even more attractive. Many systematic studies have been published on the catalytic properties of Ni-P and Ni-B catalysts [16–22], but only few reports appeared on Co-B catalyst [23–28].

In this work, we prepared amorphous Ni-B and Co-B catalysts and tested them in the hydrogenation of various unsaturated nitriles. Similar to the hydrogenation of unsaturated aldehydes, the selectivity to the desired unsaturated amine is determined by the relative accessibility and the binding strength of the C=C and C≡N bond. Therefore, a properly designed catalyst with surface sites, which invoke the polarization of the C≡N bond and inhibit the adsorption of the unsaturated nitrile in the C=C bonding configuration, can result in a high selectivity to unsaturated amine. One of the possibilities how to modify the active sites of the catalyst is the addition of a second, more electropositive metal. Therefore, Cr-doped Ni-B and Co-B catalysts were prepared in similar manner and their properties were compared with their un-doped counterparts.

As mentioned before, the presence of ammonia is essential for obtaining high selectivity to unsaturated as well as to primary amines in case of Raney catalysts [13]. It is known that ammonia interacts strongly with boron and thus, it acts as a poison for the metal boride catalysts. As an attempt to replace the ammonia and to further improve the catalyst selectivity, some of the catalysts were modified by treatment with sodium hydroxide.

In order to study the effect of chromium doping and the modification with sodium hydroxide, atomic absorption spectroscopy (AAS), nitrogen physisorption, X-ray diffraction (XRD), temperature programmed desorption (TPD), temperature programmed reduction (TPR), hydrogen chemisorption, X-ray photoelectron spectroscopy (XPS) and scanning electron microscopy (SEM) coupled with energy dispersive X-ray analysis (EDX) were used to characterize the catalysts. The results of the characterization methods were compared with the catalysts behaviour in the hydrogenation of several unsaturated nitriles.

2. Experimental

2.1. Chemicals

Cinnamonitrile (97% *trans*-), cyclohex-1-enylacetonitrile, geranylnitrile (Acros chemicals), *trans*-3-pentenenitrile, *cis*-2-pentenenitrile (Aldrich), 3,3-dimethyl-acrylonitrile (Merck), cobalt(II) acetate·$4H_2O$ (<99%), $NiCl_2 \cdot 6H_2O$ (<98%), $CrCl_3 \cdot 6H_2O$ (<98%, Fluka) and $NaBH_4$ (Fisher Scientific) were available commercially and were used as supplied.

2.2. Catalysts preparation

CoB and NiB catalysts were prepared by the chemical reduction reported by Li et al. [26]. An aqueous solution of cobalt acetate or nickel chloride was reduced with a 1-M solution of $NaBH_4$ containing 0.1-M NaOH. The molar ratio of $NaBH_4$ to Me^{2+} was kept at 5:1 to ensure complete reduction. The $NaBH_4$ solution was added dropwise while cooling with an ice bath. The mixture was vigorously stirred until no gas released. The resulting black precipitate was washed with distilled water until pH 7 and the final product was stored under distilled water. Chromium-promoted catalysts were prepared by the same method using an aqueous solution of $Co(Ac)_2$ or $NiCl_2$ and $CrCl_3$ with Me^{2+}/Cr^{3+} ratio 95:5 wt.% (Me^{2+} = Co or Ni). Part of the CoBCr catalyst was treated with NaOH solution to remove part of the boron. The CoBCr catalyst was placed into a flask and distilled water was added (15 ml of distilled water per 1 g of wet catalyst). The mixture was heated to 70 °C while stirring, then a 3-M solution of NaOH was added dropwise (20 ml) and the mixture was stirred for 90 min. The mixture was cooled down and the final precipitate was washed with distilled water to remove soluble boron species and until neutral pH was obtained. The catalyst was stored under distilled water. This preparation results in metal boride catalysts with ultra fine particles [26]. The catalyst was dried under vacuum and it was found that 600 mg of wet catalyst corresponds to 120 mg of dry mass.

2.3. Catalyst characterization

The bulk chemical composition of the prepared catalysts was analyzed by means of AAS with a Varian SpectrAA 220FS instrument. An exact amount of dry catalyst was dissolved under inert atmosphere in 20 ml of a 1:1 mixture of nitric acid and hydrochloric acid. After complete dissolution of the catalyst, the sample was diluted with distilled water to 100 ml of final solution used for analysis. The instrument was calibrated with blank sample and three standard solutions of known concentration 5, 10 and 15 μg/ml of Co^{2+}, Ni^{2+} or Cr^{3+} cation and 0.5, 1.0 and 1.5 μg/ml of Na^+ cation. An air-acetylene flame was used.

Powder X-ray diffraction (XRD) patterns of the prepared catalysts were recorded from 5° to 50° 2θ on a STOE DARMSTAD powder diffractometer using Cu Kα radiation and Ge (1 1 1) monochromator at a step size of 0.03°. A thin layer of wet catalyst was dispersed between sticking plastic films to avoid oxidation of the specimen, which was rotated continuously during the measurement. The BET surface area (S_{BET}) of the catalysts was determined by N_2 adsorption at −196 °C using a TriStar 3000 apparatus (Micromeritics).

Temperature programmed desorption measurements were carried out on a TPD apparatus (Micromeritics 2900) equipped

with TCD detector. The catalysts were pre-treated at 70 °C for 1 h in a flow of argon (25 ml/min) to remove water before the TPD measurements. The desorption of hydrogen was carried out in a flow of argon (25 ml/min) with a temperature ramp of 10 °C/min. Data were recorded from 25 to 650 °C.

Temperature programmed reduction was carried out in a flow of 4.8% H_2 in Ar (25 ml/min) from 25 to 900 °C with a heating rate of 10 °C/min. The samples of the catalysts were pre-treated by heating to 650 °C in a flow of Ar (15 ml/min) in order to remove water and species adsorbed on the catalyst surface. Then the sample was cooled to room temperature, argon was replaced by 4.8% H_2 in Ar and the TPR measurement was initiated.

Chemisorption of hydrogen was performed on an ASAP 2010 (Micromeritics) instrument. Samples were evacuated at 100 °C for 2 h, then cooled to room temperature and evacuated at RT for another hour. Evacuation was followed by leak test at room temperature. Chemisorption of hydrogen was determined by measuring the isotherm at 35 °C.

The surface morphology and the uniformity of the catalyst elemental composition was studied by scanning electron microscopy (SEM) coupled with energy dispersive X-ray analysis (EDX). The measurements were carried out on a XL30 (FEI Co., USA) electron microscope with energy dispersive X-ray spectrometer (EDX Inc., USA). The catalyst samples were transferred on an aluminium sample holder under water, the holder was placed into the electron microscope and the sample was quickly evacuated. An electron voltage of 30 keV and scanning angle of 90° were used for the measurements.

Surface elemental composition and the electronic states of Ni, Co and B were determined by X-ray photoelectron spectroscopy using a high resolution ESCA Probe P photoelectron spectrometer (Omicron Nanotechnology Ltd.). The wet samples of the catalysts were transferred to the entrance chamber of the spectrometer under water, the chamber was closed and the atmosphere was exchanged to argon. The samples were dried in a flow of argon for 2 h and then under a vacuum, until a pressure of 5×10^{-8} mbar was reached. The measurements were carried out at 5×10^{-9} mbar. Monochromatic Al Kα radiation (1486.7 eV) was used for excitation of the photoelectrons. The detector equipped with five channeltrons worked with a pass energy of 50 and 20 eV and with a step in kinetic energy of 0.5 and 0.1 eV, respectively. The photoemission lines Ni 2p, Co 2p, Cr 2p, B 1s, C 1s and O 1s were measured in high resolution mode. The spectra were calibrated with the carbon 1s peak (binding energy 284.7 eV). A low energy electron gun (1–2 eV) was used to compensate for sample charging because of the relatively high electrical resistance between the specimen and the specimen holder or because of low electrical specimen conductivity. Every sample was measured at three different states: (a) as prepared, (b) after the cleaning of the surface with an argon gun (5 keV for 30 min) and (c) after oxidation in air (sample was taken out of the spectrometer for 3 min). The measured spectra were processed by Casa XPS software. Mathematical smoothing and ''Shirley'' type of background removal were applied for quantification. The identification of the components was carried out using the NIST database and by comparison with published results [19,22,26].

2.4. Hydrogenation experiments

Hydrogenation reactions were performed in the liquid phase in a 60-ml stainless steel autoclave (Premex AG) equipped with a sampling tube and magnetic gas-inducing impeller. The catalyst (usually 120 mg of dry mass) and solvent (27 ml MeOH) were placed into the reactor and an appropriate amount of substrate (24 mmol) was added. Hydrogenation of *trans*-3-pentenenitrile was carried out with pure methanol as well as with methanol saturated with ammonia (27 wt.% of NH_3) as solvent, all the other substrates were hydrogenated only in pure methanol. The autoclave was closed, and the air was displaced first with nitrogen (three times) and then with hydrogen (three times). The autoclave was pressurized with hydrogen to the desired value (80 bar) and a leak test was carried out (10 min). The reaction was started at room temperature by turning on the magnetic stirrer (ca. 1100 rpm). After saturation of the liquid phase with hydrogen (1.5 min), the reactor was heated up to the reaction temperature (usually 12 min from 25 to 100 °C). The samples were withdrawn periodically until there was no observable consumption of hydrogen. Then the reaction was stopped, the pressure was released and the hydrogen was displaced by nitrogen. Withdrawn samples and product were filtered in order to remove the catalyst and analyzed by gas chromatography on a Agilent GC (HP6890 equipped with autosampler and semipolar chromatographic column DB-17, 30 m × 0.32 mm × 0.5 μm from J&W Scientific) under the following conditions: carrier gas, helium 113.5 kPa; temperatures, inj. 250 °C, det. 280 °C; oven temperature program, 50 °C (5 min), 30 °C/min to 280 °C (10 min). The products were characterized by comparison of their retention times with corresponding analytical standards.

3. Results and discussion

3.1. Catalysts characterization

Chemical reduction of transition metal ions by the reaction with $NaBH_4$ leads to ultra fine particles of amorphous alloys [29–31]. The composition of such materials is strongly dependent on the reduction conditions. Usually three types of compounds are generated during reduction: metals, metal borides and metal borates (Me, Me_2B and $Me(BO_2)_2$, respectively). Reduction in aqueous media results in Me_2B as primary product. However, in order to obtain the pure Me_2B particles, the procedure has to be carried out under anaerobic conditions [29–31]. If the reduction is performed in the aqueous media under a normal atmosphere (as in our case), metal borates and boron oxide can be formed as side products [26,32]. The chemical composition of the prepared catalysts, as determined by AAS, shows that the majority of the catalyst is formed by the transition metal (Table 1). After doping with chromium, the content of transition metal decreases in favour of boron and oxygen. The almost double concentration of the sum

Table 1
Chemical composition and BET surface area of prepared catalysts

Catalyst	Ni (wt.%)	Co (wt.%)	Cr (wt.%)	Σ (B,O) (wt.%)	S_{BET} (m^2/g)
NiB	86			14.0	40
NiBCr	73		1.3	25.7	49
CoB		90		10.0	19
CoBCr		75	1.1	23.9	40
CoBCr-Na[a]		69	1.2	29.8	27 (24%)[b]

[a] Na concentration <1 wt.%.
[b] Metal area.

of boron and oxygen in the Cr-promoted catalysts implies a larger presence of borates and boron oxide. The AAS analysis of the CoBCr-Na catalyst, which was treated with a saturated NaOH solution, showed a slight decrease of the cobalt content in comparison with the CoBCr catalyst. This suggests that besides removal of part of the boron oxide from the surface, also hydrolysis of Co_2B occurs, which is facilitated by higher temperature [31]. Removal of boron species and its transformation into sodium borate was also indicated by a change of the color of the solution, which turned green-brown, and by enhanced magnetic properties of the residual precipitate. The Na-concentration in the CoBCr-Na catalyst measured by AAS was below 1 wt.%, proving that the sodium is completely washed out and does not deposit on the catalyst. The concentration of chromium in the Cr-doped catalysts ranged from 1.1 to 1.3 wt.%. All three Cr-doped catalysts showed an increased total surface area in comparison with the un-doped NiB and CoB catalysts (Table 1). In case of CoB, the total surface area increased even by factor of 2 (from 19 to 40 m^2/g). It has been already shown [22] that the addition of chromium can reduce the particle size of nickel boride and thus increase the surface area of the catalyst. It seems that the same effect is observed with the cobalt catalysts. The direct evidence of the chromium effect on the particle size obtained by SEM will be discussed below. The increase of the total surface area is also related to the higher contents of boron and oxygen in the Cr-doped catalysts and thus to the presence of borates and boron oxide. The treatment of the CoBCr catalyst with sodium hydroxide caused a decrease of the surface area by about 30%, probably because part of the boron compounds was removed by washing with NaOH.

Fig. 1 shows the XRD diffraction patterns of the prepared catalyst samples. The XRD spectra of the NiB and NiBCr catalysts contained besides an amorphous phase also features of crystalline material [19,32]. While a broad diffraction line at 45° 2θ corresponds to crystalline metal boride [19], the second broad diffraction line at 27° 2θ indicates the presence of amorphous boron oxide [26]. On the other hand, the completely amorphous structure of CoB and CoBCr catalysts was confirmed.

The surface morphology studied by SEM demonstrated a broad particle size distribution of the prepared NiB and CoB catalysts. Rather large compact particles accompanied by smaller particles could be observed in the samples of NiB (Fig. 2a) and CoB (not shown). On the other hand, the catalysts doped with chromium consisted of smaller particles and their particle size distribution was much more uniform (Fig. 2b). Chromium seems to reduce the particle size of the NiB as well as CoB catalysts, in agreement with the higher surface areas of both Cr-doped catalysts (Table 1). The morphology of the CoBCr-Na catalyst was very similar to that of CoBCr. The chemical composition of the catalysts obtained by EDX microanalysis (Table 2) was measured at three different spots on each catalyst. The differences in chemical composition measured at different spots were less than 10%. Table 2 shows the average values of these three measurements. The boron concentrations were low and may therefore contain a relatively high experimental error. However, the sum of boron and oxygen and the concentrations of the other elements correspond well with the AAS results. It was confirmed that chromium doping results in lower nickel and cobalt concentrations and higher concentrations of boron and especially oxygen. This suggests that the reduction of the transition metal in the presence of chromium provides higher contents of borates and boron oxide. Further treatment of the CoBCr catalyst with a saturated NaOH solution decreased the cobalt as well as boron concentrations, while the concentration of oxygen was increased. The distribution of chromium was measured at different spots on the catalysts and it was found that chromium is homogeneously dispersed.

All these results clearly suggest different ratios among Me_2B, $Me(BO_2)_2$ and B_2O_3 in all individual samples. In the CoB catalyst, cobalt is mainly present as cobalt boride accompanied by a very small portion of cobalt borate and

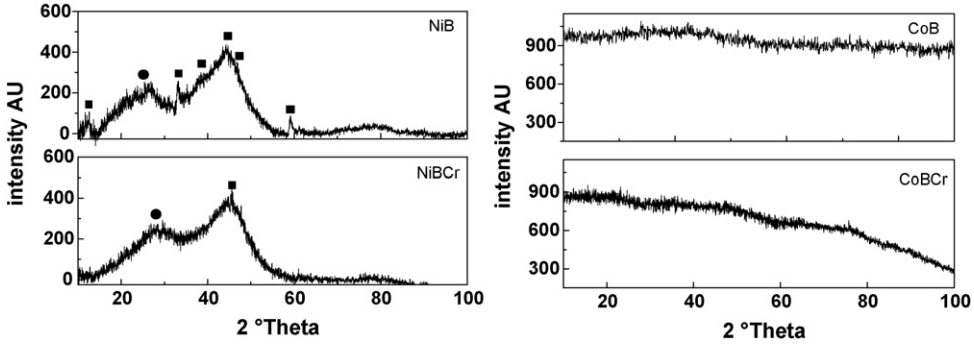

Fig. 1. XRD spectra of nickel and cobalt borides compared with their chromium doped equivalents: (■) diffraction lines of crystalline Ni_2B, (●) broad line of amorphous B_2O_3.

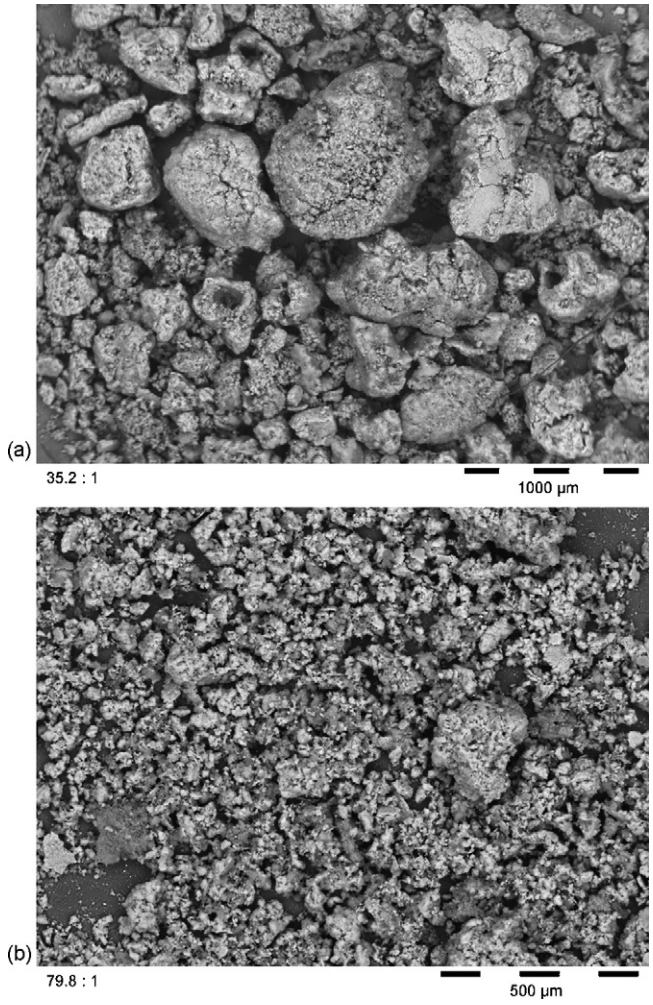

Fig. 2. SEM images of the (a) NiB and (b) NiBCr catalysts.

boron oxide. In the NiB catalyst, more nickel borate and boron oxide is probably present. Chromium-doped catalysts exhibit a several times higher concentration of oxygen implying a higher concentration of metal borates and boron oxide.

To find out more about the composition of the catalysts and to differentiate among borides, borates, and boron oxide, XPS was used to analyze the catalysts. First spectra were measured in the binding energy range from 0 to 1300 eV. The samples contained all expected elements (Ni, Co, Cr, O and B) and also a small amount of carbon impurity. No traces of sodium were detected in the catalysts. The total stoichiometry of the surface layer was calculated from the integral intensities of the spectral lines adjusted to the partial photo-ionization cross-sections (Table 3). The results are in line with those obtained by AAS and EDX. All the catalysts contain a similar amount of boron and the addition of chromium lowers the metal and increases the oxygen contents. Sodium hydroxide treatment of the CoBCr catalyst further decreased the level of cobalt and increased the level of oxygen.

Table 2
Chemical composition of the catalysts measured by SEM-EDX

Catalyst	Ni (wt./at.%)	Co (wt./at.%)	Cr (wt./at.%)	B (wt./at.%)[a]	O (wt./at.%)
NiB	82/52			5.6/19.3	12.4/28.8
NiBCr	72/39		2.0/1.1	7.8/23.1	18.2/36.4
CoB		91/67		6.2/25.0	2.8/7.6
CoBCr		81/51	2.1/1.5	8.8/28.3	11.1/24.2
CoBCr-Na[b]		77/46	2.6/1.6	8.1/24.1	17.3/34.9

[a] Data of boron are based on relatively low net vs. total intensity ratios and therefore they may contain a relatively high experimental error.
[b] Na-concentration was bellow detection limit (<0.5 wt.%).

The Ni $2p_{3/2}$ spectra of the NiB and NiBCr catalysts consisted of a major peak at 852.3 eV, which corresponds to pure metallic nickel (852.8 eV), and of a small peak at higher binding energy (855.5 eV), which corresponds to Ni^{2+} ions (856.2 eV). The ratio of the metallic nickel (Ni^0) and nickel ion (Ni^{2+}) peaks was 95:5 (Table 3), showing that the majority of nickel was present in metallic form. The 1s spectrum of boron was more complicated and exhibited at least three different components. A well-separated peak of metallic boron (B^0) was present at 189.2 eV. The other two components corresponding to B^{3+} species overlapped and formed a broad peak with a maximum around 193.5 eV. The broad peak ascribed to borate species (BO_2^-) and boron oxide (B_2O_3), was deconvoluted and the ratio of the components together with their maxima was obtained (Table 3). Comparing standard binding energies of pure elemental Ni (852.8 eV) and B (187.5 eV) with those obtained for alloyed Ni and B in NiB and NiBCr samples reveals that the binding energy of metallic Ni present in the alloy is negatively shifted by approximately 0.5 eV, while the binding energy of alloyed B is shifted positively by 1.7 eV. This implies the electron transfer from elemental boron to metallic nickel in the NiB amorphous alloys [19,22], making the metallic nickel electron enriched and the alloyed B electron deficient.

In the NiB catalyst, the majority of boron was present in metallic form and the ratio between borate species and boron oxide was approximately 1:1. After the chromium addition, the component corresponding to metallic boron (B^0) decreased 50% in intensity and the oxidized boron species (BO_2^- and B_2O_3) increased accordingly. The positions of the Ni 2p and B 1s signals changed only slightly by adding chromium and these small shifts (±0.3 eV) were within the experimental error of the measurements. Therefore, it seems that the presence of Cr does not modify the electronic interactions between Ni and B.

Similarly, two components were present in the Co $2p_{3/2}$ spectra of the cobalt catalysts. The major peak at 778.0 eV corresponds to metallic cobalt (Co^0), while the less abundant peak at 781.0 eV is characteristic for divalent cobalt ions (Co^{2+}). In this case, the negative shift of the binding energy of metallic cobalt in the CoB alloy is almost negligible (−0.2 eV). Also the positive shift in binding energy of B^0 (approximately +0.7 eV) was lower than in case of the NiB catalyst. Moreover, the binding energies of the borate (BO_2^-) and the boron oxide (B_2O_3) components were lower than in case of the nickel catalyst. This could mean that the partial electron transfer from the alloyed B^0 occurs to the neighbouring oxygen present in the form of boron oxide rather than to metallic Co^0, because the

Table 3
Stoichiometry and the components distribution of the catalysts surface layer

Catalyst	Composition (at.%)	Ni 2p (eV)		Co 2p (eV)		B 1s (eV)[a]		
		Ni^0	Ni^{2+}	Co^0	Co^{2+}	B^0	BO_2^-	B_2O_3
NiB	$Ni_{56}B_{24}O_{20}$	852.3 (95)	855.5 (5)			189.2 (58)	192.9 (22)	193.9 (20)
NiBCr	$Ni_{39}Cr_{3.6}B_{22}O_{35.4}$	852.5 (93)	854.9 (7)			189.1 (26)	193.1 (39)	194.2 (35)
CoB	$Co_{68}B_{21}O_{11}$			778.0 (88)	781.0 (12)	188.2 (63)	191.9 (20)	193.0 (17)
CoBCr	$Co_{42}Cr_{2.4}B_{25}O_{30.6}$			778.2 (73)	781.2 (27)	188.3 (22)	192.2 (37)	193.1 (41)
CoBCr-Na	$Co_{34}Cr_{3.1}B_{23}O_{39.7}$			778.2 (83)	780.7 (17)	188.5 (35)	192.3 (29)	193.4 (36)

oxygen is more electronegative. However, the binding energy shifts are rather small to really prove the electron transfer from boron to cobalt and/or oxygen.

The addition of chromium had a similar effect on the Co^0:Co^{2+} ratio as in the case of the nickel catalyst: the content of Co^{2+} species increased to the detriment of metallic cobalt (Co^0). At the same time, the component corresponding to metallic boron (B^0) decreased to almost one third of its original intensity and the oxidized boron species (BO_2^- and B_2O_3) increased accordingly. The NaOH treatment of the CoBCr catalyst had the opposite influence on the Co^0:Co^{2+} ratio as the Cr doping and the original ratio of Co^0:Co^{2+} (as in CoB catalyst) was almost regained. Part of the cobalt borate ($Co(BO_2)_2$) probably dissolved and was washed out from the catalyst during the NaOH treatment. This is supported not only by the fact that the Co^{2+} content decreased after the treatment, but also by the decreased borate (BO_2^-) content.

The chromium 2p spectrum displayed two peaks: one at 576.8 eV (ascribed to Cr $2p_{3/2}$) and a second, lower and broader one, at 587.3 ± 0.7 eV (overlapped Cr $2p_{1/2}$ peak and the satellite peak of Cr $2p_{3/2}$). This pattern is characteristic for Cr^{3+} species [33] and thus, we ascribed it to Cr_2O_3. Since the effect of the chromium addition on the binding energies of Ni, Co and B was very small (within the experimental error), the presence of chromium probably does not modify the electronic interactions between Ni-B and Co-B significantly. The higher Cr concentrations measured at the catalyst surface layer in comparison with those obtained from the bulk (Tables 1–3) suggest that Cr^{3+} species, most probably in the form of Cr_2O_3, are occluded at the surface of the catalysts. The presence of this surface oxide layer helps to keep the metal boride particles separated, because otherwise they would agglomerate due to their high surface energy [22]. This leads to the lower particle size of the Cr-doped boride catalysts and to their higher surface areas.

Fig. 3 shows the temperature programmed desorption spectra of hydrogen of all catalysts. The catalysts were pretreated at 70 °C for 1 h to remove water before the measurement. It was observed that the higher pretreatment temperatures cause structural changes of the catalysts (crystallization, decrease of the surface area) and, thus, the consecutive TPD measurements provide information only about hydrogen, which can be reversibly adsorbed on the surface. Although the used temperature was not sufficient to remove the water completely, the residual content of water was negligible in comparison to the amount of hydrogen adsorbed and absorbed by the catalysts. The desorption spectrum of the NiB catalyst exhibits two bands with maxima at 143 and 320 °C, showing the presence of two types of hydrogen species (weakly and strongly bonded hydrogen). Modification of the NiB catalyst with chromium caused a dramatic change in the ratio of these two types of hydrogen with a significant increase in the amount of weakly bonded hydrogen. Chromium also shifted the desorption maxima of both desorption bands to lower temperatures. Weakly bonded hydrogen desorbed at 127 and 143 °C for the NiBCr and NiB catalysts, respectively. The strongly bonded hydrogen desorbed at 290 °C from the NiBCr catalyst and above 320 °C from the NiB catalyst. The unmodified cobalt boride catalyst showed only one desorption band at 153 °C with a long tail continuing till 400 °C. This band can be ascribed to the removal of surface hydrogen followed by the desorption of hydrogen from subsurface layers at higher temperatures. These results are consistent with the results of AAS, EDX and XPS and show the homogeneity of the unmodified cobalt boride sample, which contains only negligible amounts of boron oxide and cobalt borates. The

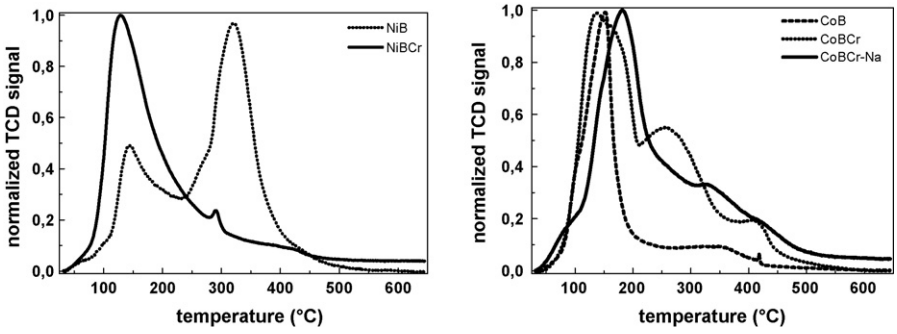

Fig. 3. Hydrogen TPD spectra of prepared catalysts.

higher concentrations of boron oxide and cobalt borates would otherwise have an impact on the profile of the CoB desorption spectra. The hydrogen desorption spectrum of the cobalt boride catalysts modified with chromium (CoBCr) is more complicated. Modification with chromium caused dramatic changes in the surface morphology indicated by the presence of four different types of hydrogen desorbing at 134, 165, 257 and 409 °C. The first band seems to be composed of two overlapping desorption events. The binding energy of hydrogen at the surface is lowered by the presence of chromium adjacent to cobalt boride and hydrogen desorbs at low temperature (134 °C). On the contrary, the desorption of hydrogen bonded to un-doped cobalt boride is shifted to higher temperature (165 °C). A new desorption band at 257 °C confirms the presence of boron oxide and cobalt borates, which have an impact on the binding energy of hydrogen in CoBCr catalyst. As in the previous case, the desorption band above 350 °C can be attributed to the removal of hydrogen from subsurface layers. The desorption spectrum of CoBCr-Na (treated with sodium hydroxide) showed in comparison with CoBCr an almost complete disappearance of weakly bonded hydrogen and a shift of the second desorption band to higher temperature (190 °C). The intensity of the desorption band at 257 °C decreased significantly as well. The TPD profiles of the CoBCr-Na catalyst became similar to the spectra of the unmodified CoB sample, proving the removal of boron oxide and a part of Co_2B from the surface. The disappearance of weakly bonded hydrogen suggests the preferential hydrolysis of cobalt boride with adjacent chromium.

Significant differences in the morphology of the un-doped and chromium-doped nickel and cobalt boride catalysts were observed during temperature programmed reduction (Fig. 4). $Ni(BO_2)_2$, $Co(BO_2)_2$ and Cr_2O_3 represent reducible species present in the prepared catalysts. Due to the positive standard free energy (ΔG^0) of Ni^{2+}, Co^{2+} and Cr^{3+}, their reduction occurs at high temperature (>300 °C) [34–40]. Thus, the bands at lower temperature (<300 °C) can be ascribed to reversible adsorption of hydrogen. On the contrary, the peaks at very high temperatures probably originate from the reduction in subsurface layers and/or in the bulk of the catalysts. The reduction profile of the NiB catalyst showed a very low hydrogen consumption below 300 °C, while the NiBCr catalyst exhibited a broad band with a maximum at 190 °C. Both bands correspond to the reversible hydrogen adsorption on nickel boride surface. One can see that the positions of the bands in the TPR spectra of hydrogen reversibly adsorbed on the surface correspond to positions of the bands in the TPD spectra of the nickel samples (cf. Figs. 3 and 4). Two bands of the NiB catalyst, occurring at high temperature (520 and 570 °C), were ascribed to reduction of Ni^{2+}. The reduction of Ni^{2+} occurs, however, just above 300 °C [34,35]. Thus, the shift to such high temperatures has to be the result of the presence of boron oxide, which dramatically affects the reducibility of this species. In the case of the chromium-doped nickel catalyst, where a higher amount of boron oxide is present, the bands are even more shifted to higher temperatures. Reduction of Cr^{3+} to Cr^{2+} exhibits the highest standard free energy and thus, the reduction occurs at very high temperature. Besides the interaction of boron oxide with Ni^{2+} species, which results in decreased reducibility, the high surface coverage with boron oxide constrains the reduction process in general.

The reduction profiles of the CoB and CoBCr catalysts exhibit three and four hydrogen consumption bands, respectively. The reduction bands below 200 °C are ascribed to reversible hydrogen adsorption on the surface of cobalt boride. The low-temperature band is followed by increased hydrogen consumption at 330 and 355 °C for CoB and CoBCr, respectively, probably as a result of Co^{2+} to Co^0 reduction. The substantially lower intensity of this band for CoB clearly indicates a lower concentration of cobalt borates, in agreement with previous results (Tables 1–3) and with TPD measurements. A new band at 450 °C in the CoBCr TPR profile can be ascribed to the reduction of Cr^{3+} to Cr^{2+}. The reduction profiles of the CoBCr-Na and CoBCr catalysts show similar shape and are both composed of four bands. Treatment of CoBCr with sodium hydroxide caused significant changes on the catalyst surface indicated by a dramatic decrease of hydrogen consumption at low temperature and its shift to substantially higher temperature (360 °C). Also the following two bands of Co^{2+} and Cr^{3+} reduction are shifted to higher temperatures, 500 and 620 °C, respectively. As in the case of the nickel catalysts, the presence of boron oxide decreased the reducibility of the Co^{2+} and Cr^{3+} species. The unchanged position of the band at 650 °C after the treatment with sodium hydroxide is probably the result of hydrogen diffusion into the bulk of the catalysts. These results suggest that boron oxidation occurs and that metal borates and boron oxide are formed during the catalyst preparation. Thus, the borates and boron oxide are present not only at the surface but also within the bulk of the catalyst.

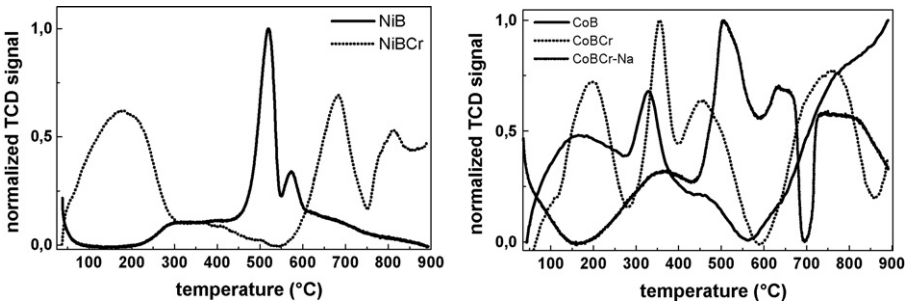

Fig. 4. Temperature programmed reduction profiles of nickel and cobalt borides and their chromium doped equivalents.

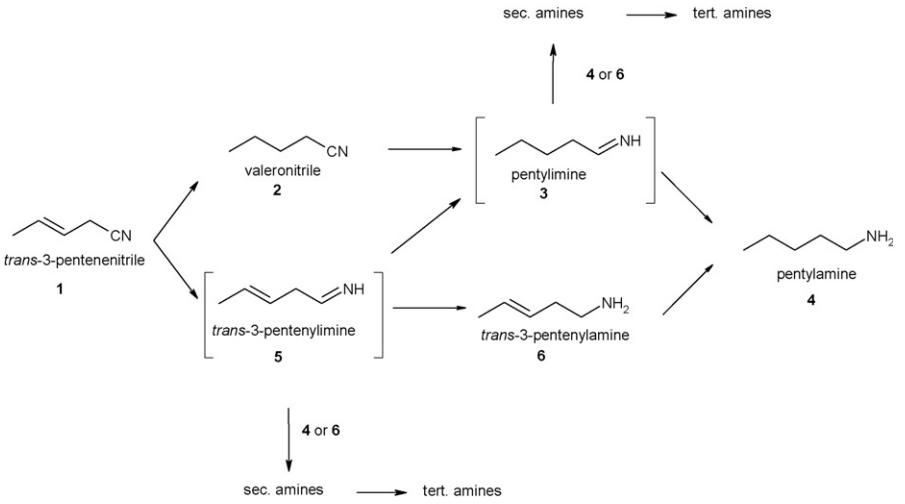

Fig. 5. Reaction scheme of *trans*-3-pentenenitrile hydrogenation.

3.2. Catalytic experiments

3.2.1. Hydrogenation of trans-3-pentenenitrile over NiB, CoB and their Cr-doped equivalents

The catalysts were tested in the hydrogenation of *trans*-3-pentenenitrile, the hydrogenation of which was already investigated in our previous study on the structure–selectivity relationship in the hydrogenation of unsaturated nitriles [9]. *Trans*-3-pentenenitrile was chosen because it contains a double bond, which is neither sterically hindered nor conjugated with another group. These features make the hydrogenation of *trans*-3-pentenenitrile more sensitive to changes in the catalyst or reaction conditions. Therefore, the molecule of *trans*-3-pentenenitrile is an ideal model substrate to explore the catalyst properties in the hydrogenation of unsaturated nitriles. The hydrogenation of *trans*-3-pentenenitrile proceeds by two different pathways (Fig. 5). In the first pathway, the double bond of *trans*-3-pentenenitrile **1** is reduced to valeronitrile **2**, which is transformed via imine **3** to the final product, pentylamine **4**. In the second pathway, the nitrile group is reduced first to the unsaturated imine **5**, which can either react to imine **3** or to the desired *trans*-3-pentenylamine **6**. Consecutive hydrogenation of **6** provides the same final product as in the first pathway, the fully hydrogenated pentylamine **4**. Furthermore, the two imine intermediates **3** and **5** can react with already formed amines **4** and **6** to form various secondary and tertiary amines. However, under optimized conditions, which were described in detail in our previous publications [9,13], the formation of secondary and tertiary amines was suppressed and their concentration did not exceed 5 wt.%. The imines **3** and **5** are very reactive intermediates and they were not observed in the reaction mixture.

The reaction course of *trans*-3-pentenenitrile hydrogenation over NiB and NiBCr catalysts is shown in Fig. 6. The *trans*-3-pentenenitrile **1** is hydrogenated first to the saturated nitrile **2** (valeronitrile), which reacts further to the fully saturated product, pentylamine **4**. The concentration profile of the unsaturated amine **6** (*trans*-3-pentenylamine) remained almost flat and its concentration did not exceed 2%. These results are in contrast to hydrogenation of **1** over Raney nickel and Raney nickel doped with chromium in methanol saturated with ammonia [9], where the reaction mainly proceeded via the unsaturated amine **6**. This difference clearly shows that the presence of ammonia influences not only the selectivity to primary amines, but also significantly affects the chemoselectivity to unsaturated amines. It is known that C=C bond hydrogenation is slowed down in the presence of nitrogen-containing compounds as well as in the presence of ammonia. Therefore, in the presence of ammonia, the nitrile group of **1**,

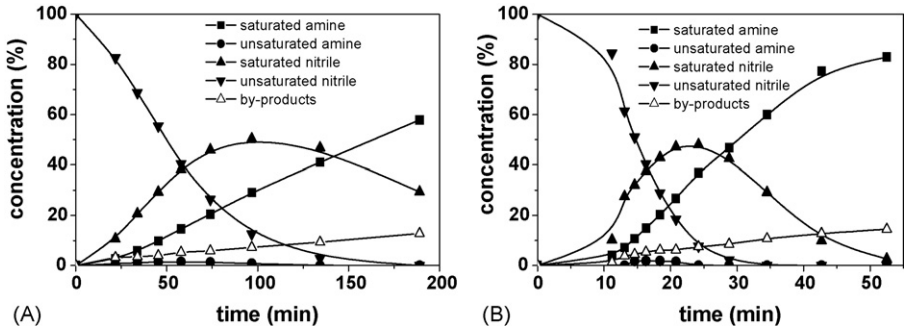

Fig. 6. Reaction profiles of *trans*-3-pentenenitrile hydrogenation in methanol over: (A) NiB and (B) NiBCr catalysts.

Table 4
Results of *trans*-3-pentenenitrile hydrogenation

Catalyst	$Rate_{50\%}$ (mmol/min g_{cat})	$SEL_{90\%}$[c]	Unsat. amine[d] (wt.%)	Sat. nitrile[e] (wt.%)	Conversion[e] (%)
NiB[a]	2.1	0.01/0.63[f]	<2	50	87
NiB[b]	0	–	–	–	–
NiBCr[a]	6.6	0/0.57[f]	<1	48	92
NiBCr[b]	0	–	–	–	–
CoB[a]	2.9	0.35	27	5	100
CoB[b]	2.1	0.38	32	14	88
CoBCr[a]	3.8	0.25	26	4	80
CoBCr[b]	2.5	0.29	25	22	92
CoBCr-Na[a]	2.7	0.53	46	3	95
CoBCr-Na[b]	1.7	0.50	44	8	93

Reaction conditions: 24 mmol substrate, 120 mg catalyst (dry mass), 27 ml solvent, 100 °C, 8 MPa of hydrogen.
[a] Solvent MeOH.
[b] Solvent 27 wt.% NH_3 in MeOH.
[c] $SEL_{90\%}$ = % unsaturated amine/(% unsaturated amine + % saturated nitrile + % saturated amine) at 90% conversion.
[d] At maximum concentration.
[e] At maximum concentration of unsaturated amine.
[f] Selectivity to saturated nitrile (valeronitrile).

which strongly adsorbes at the surface of the catalyst, is hydrogenated first and the double bond remains untouched as long as the nitrile is present in the reaction mixture. On the other hand, in the system without ammonia, the C=C bond can adsorb at the surface of the catalyst and is hydrogenated preferentially (before the C≡N group) because of thermodynamics. Moreover, the results show that the NiB and NiBCr catalysts are very active in double bond hydrogenation. This can be related to the higher amount of weakly bonded hydrogen present in NiB and NiBCr catalysts in comparison to commercial Raney nickel catalyst (unpublished results) applied in previous publication [9].

Table 4 shows the results of *trans*-3-pentenenitrile hydrogenation over all prepared catalysts. The activity of the catalysts is presented as the reaction rate at 50% conversion of **1**. The selectivity to unsaturated amine was defined as $SEL_{90\%}$ = % unsaturated amine/(% unsaturated amine + % saturated nitrile + % saturated amine) and was calculated at 90% conversion of **1**. The concentration of unsaturated amine **6** represents the highest concentration of **6** (*trans*-3-pentenylamine) reached during the reaction. This maximum concentration was reached at the conversion shown in the last column. At the same conversion, the concentration of saturated nitrile **2** (valeronitrile) is shown. The sum of by-products including secondary and tertiary amines did not exceed 10% (at the maximum concentration of the intermediate). The addition of ammonia was tested with all prepared catalysts, but it resulted in lower activity (in case of the nickel catalysts the activity was even zero) and in case of the cobalt catalyst also in lower selectivity to unsaturated amine **6**. The ammonia interacts strongly with boron species at the catalyst surface, blocks the active sites and thus decreases the activity of the catalysts. The interaction between boron species and ammonia seems to be much stronger for the nickel than cobalt catalysts.

Fig. 6 shows that the hydrogenation of *trans*-3-pentenenitrile proceeds via the saturated nitrile **2** (valeronitrile) over NiB as well as over NiBCr. The doping with chromium results mainly in higher activity of the catalyst, which increased more than three times (see Fig. 6 and Table 4). The influence of Cr-doping on selectivity was negligible.

The CoB and CoBCr catalysts were active in methanol as well as in methanol saturated with ammonia. The reaction rate of the CoB catalyst was higher than that of NiB, but after doping with chromium the increase in activity was not as noticeable as in case of NiBCr (Table 4). The main difference between the nickel and cobalt catalyst is the different product distribution. While the hydrogenation of **1** proceeds via the saturated nitrile **2** over the nickel catalysts, the hydrogenation over the cobalt catalysts occurs preferentially via the unsaturated amine **6** (Fig. 7). The low maximum concentrations of unsaturated amine and relatively low selectivity (Table 4) are a consequence of the rapid consecutive hydrogenation of the

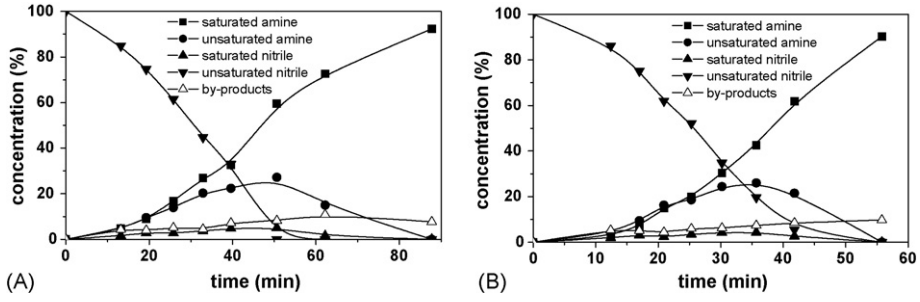

Fig. 7. Reaction profiles of *trans*-3-pentenenitrile hydrogenation in methanol over (A) CoB catalyst (B) CoBCr catalysts.

C=C double bond to the saturated amine **4**. The rapid drop of selectivity at higher conversions was even more pronounced after the chromium doping. The selectivity to unsaturated amine over CoBCr was higher than that over CoB (0.44 versus 0.40) at 50% conversion of **1**, however, at higher conversion, the selectivity over CoBCr decreased rapidly (0.25 at 90% conversion) due to the fast consecutive hydrogenation of **6** to **4**. Nevertheless, the concentration of saturated nitriles was always below 5% over both CoB and CoBCr catalysts.

Using methanol saturated with ammonia instead of pure methanol did not increase the selectivity towards the unsaturated amine over CoB. The consecutive hydrogenation of the C=C bond of the unsaturated amine **6** was slightly suppressed, but a higher concentration (up to 14%) of saturated nitrile **2** was obtained. The slight effect of ammonia on the catalytic activity and selectivity can be explained by the homogeneity of the catalyst composed mainly of Co_2B, with negligible amount of borate and boron oxide. Using methanol saturated with ammonia in case of CoBCr decreased the selectivity to unsaturated amine (0.30 at 50% conversion) due to the simultaneous hydrogenation of the C=C bond of the unsaturated nitrile **1** and as a consequence up to 24% of the saturated nitrile **2** was obtained. The higher content of boron oxide and borates in comparison to the CoB catalyst results in a more significant drop of the catalytic activity due to a strong interaction of ammonia with boron oxide and/or borate.

3.2.2. *Hydrogenation of unsaturated nitriles over CoBCr treated with NaOH*

The activity of CoBCr treated with sodium hydroxide (CoBCr-Na) was lower than with CoBCr, but comparable to the un-doped CoB catalyst. Nevertheless, the CoBCr-Na catalyst exhibited the highest selectivity to unsaturated amine of all catalysts studied: 0.64 at 50% conversion and 0.53 at 90% conversion (Table 4). The concentration of unsaturated amine reached its maximum (46%) at 95% conversion and, at the same conversion, the concentration of saturated nitrile was only 3%. Much lower activity and slightly lower selectivity, 0.57 at 50% conversion and 0.50 at 90% conversion, was obtained in ammonia saturated methanol.

The treatment with NaOH at elevated temperature probably not only caused the removal of borates and boron oxide species from the surface of the catalyst but also the removal of weakly bonded hydrogen. This is supported by the TPD results, which

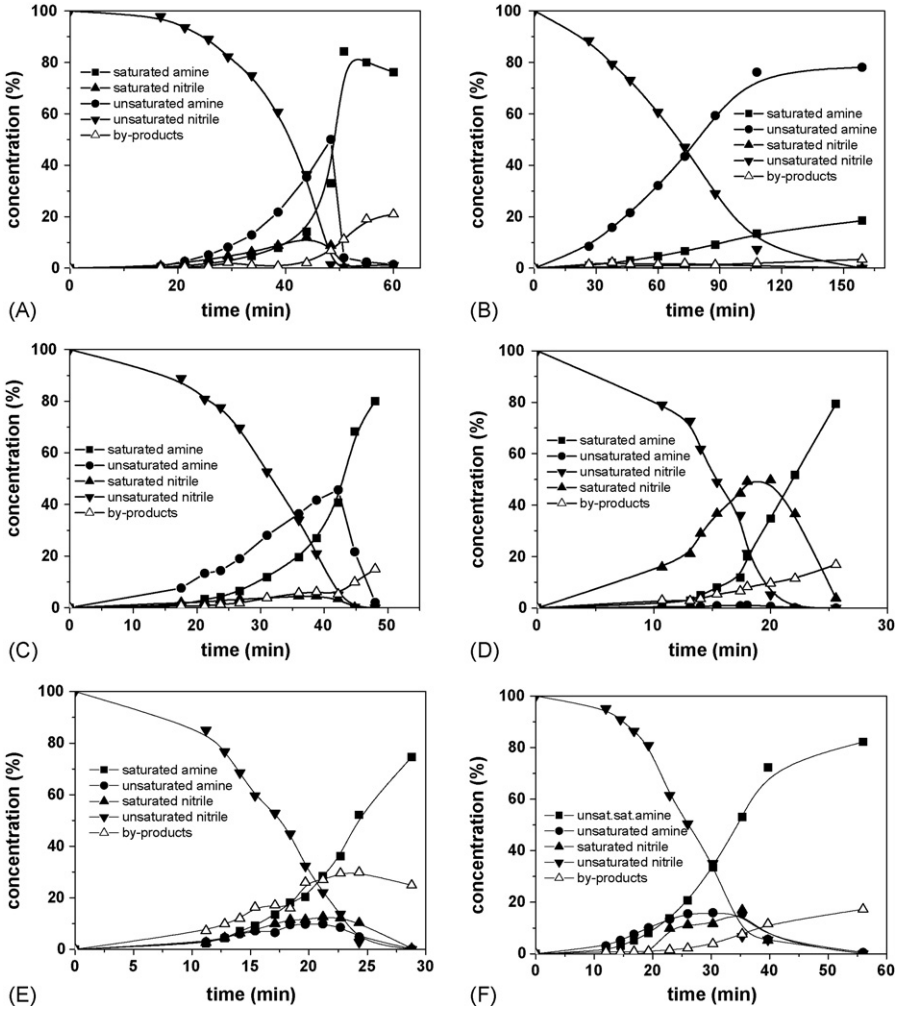

Fig. 8. Reaction profiles of hydrogenation of different substrates over CoBCr-Na catalyst: (A) cinnamonitrile, (B) 1-cyclohexenyl-acetonitrile, (C) *trans*-3-pentenenitrile, (D) *cis*-2-pentenenitrile, (E) 3,3-dimethyl-acrylonitrile and (F) geranylnitrile.

confirmed the disappearance of weakly bonded hydrogen and showed that the second desorption band of CoBCr-Na was shifted to higher temperature (190 °C). The disappearance of weakly bonded hydrogen suggests the preferential hydrolysis of boride species with adjacent chromium, resulting in the formation of isolated Cr_2O_3 species. The active site of the catalyst can then be formed by cobalt boride particles partly covered with chromium oxide and with almost no weakly bonded hydrogen, which is responsible for non-selective C=C bond hydrogenation.

According to the adsorption model of the nitrile [12], the electronic interaction between the C≡N group and the metallic active sites was the forward donation of the electrons from the highest occupied molecular orbital (HOMO) of the C≡N bond and the back donation from the metal $d_{xz,yz}$ states to the lowest unoccupied molecular orbital (LUMO) of the C≡N bond. Increased back donation may favour the C≡N bond dissociation since the LUMO is an anti-bonding orbital. Thus, from the hydrogenation point of view, an increase in electron density on Co due to the electron transfer from boron (suggested by the XPS results) should lead to increased back donation to the LUMO, i.e. π^*_{CN}, thereby weakening the C≡N bond, which in turn should favour the hydrogenation. When the π^*_{CN} orbital is shifted down, the interaction of the C≡N bond with the metallic site is facilitated and the adsorption is stronger. The shift of the π^*_{CN} orbital to lower energy can be achieved by complexation of the nitrile group with a Lewis acid [41]. The Cr^{3+} species present at the catalyst surface could act as Lewis adsorption sites and the nitrile molecule can be adsorbed via donation of the lone pair from the nitrogen of the nitrile group. This bonding polarizes the nitrile group, which is favourable for a nucleophilic attack on the carbon atom by hydrogen dissociatively adsorbed on neighbouring active Co sites. The presence of surface chromium oxide can, therefore, improve the adsorption and the reactivity of the nitrile group, which explains the higher activity obtained over Cr-doped catalysts.

To fully explore the properties of the CoBCr-Na catalyst, several substrates with conjugated as well as with non-conjugated and differently substituted double bonds were selected and their hydrogenation was studied. Fig. 8 shows the reaction course of cinnamonitrile, 1-cyclohexenyl-acetonitrile, *trans*-3-pentenenitrile, *cis*-2-pentenenitrile, 3,3-dimethyl-acrylonitrile and geranylnitrile over the CoBCr-Na catalyst in methanol. The highest selectivities to unsaturated amine were obtained with cinnamonitrile (due to the stabilization effect of the phenyl ring conjugation with the C=C bond), 1-cyclohexenyl-acetonitrile (due to the sterically hindered C=C bond present in the cyclohexane ring) and with *trans*-3-pentenenitrile (due to the remote position of the double bond, which was not in conjugation with the nitrile). The highest concentration of unsaturated amine (78%) was reached with 1-cyclohexenyl-acetonitrile (Table 5). A slightly lower maximum concentration was obtained with cinnanonitrile and *trans*-3-pentenenitrile. The hydrogenation of *cis*-2-pentenenitrile proceeded purely via the saturated nitrile (Fig. 8D), because the double bond of *cis*-2-pentenenitrile is conjugated and activated by the nitrile group and there is no sterical hindrance. The conjugated C=C and C≡N π-bonds of *cis*-2-pentenenitrile probably adsorb at the surface and the activated C=C bond is hydrogenated preferentially. The higher reactivity of a conjugated and not sterically hindered double bond is also demonstrated by the much higher reaction rate of *cis*-2-pentenenitrile (Table 5). The 3,3-dimethyl-acrylonitrile and geranylnitrile, which posses a conjugated double bond with the nitrile group and differ only by in the size of the double bond substituent, provided lower selectivity because of rapid consecutive hydrogenation of the C=C and C≡N bonds (Fig. 8E and F). A higher amount of by-products was formed during the hydrogenation of 3,3-dimethyl-acrylonitrile. They consist mainly of secondary imines and amines formed at high reaction temperature. However, in all other cases, the concentration of by-products at the maximum concentration of unsaturated amine did not exceed 10%. It should be noted that this high selectivity to primary amines was obtained without any addition of a base to the reaction system! If we compare the results with those of *cis*-2-pentenenitrile, which posses only one substituent (ethyl group) at the double bond, it is obvious that the presence of the additional methyl group at the double bond in 3,3-dimethyl-acrylonitrile and geranylnitrile is responsible for the selectivity increase. The lower reaction rates of 3,3-dimethyl-acrylonitrile and geranylnitrile in comparison with *cis*-2-pentenenitrile provide further evidence of steric hindrance of the double bond by the second methyl group present in the molecule (Table 5).

Table 5
Results of hydrogenation of various substrates over CoBCr-Na catalyst

Substrate	$Rate_{50\%}$ (mmol/min g_{cat})	$SEL_{50/90\%}$[a]	Unsat. amine[b] (wt.%)	Sat. nitrile[c] (wt.%)	Conversion[c] (%)
Cinnamonitrile	2.5	0.57/0.55	50	9	99
1-Cyclohexenyl-acetonitrile	1.4	0.85/0.81	78	0	100
trans-3-Pentenenitrile	2.7	0.64/0.53	46	3	95
cis-2-Pentenenitrile	7.1	0.84[d]/0.58[d]	0.02	50	95
3,3-Dimethyl-acrylonitrile	3.3	0.22/0.06	8	13	70[e]
Geranylnitrile	3.8	0.33/0.07	16	16	65

Reaction conditions: 24 mmol substrate, 120 mg catalyst (dry mass), 27 ml MeOH, 100 °C, 8 MPa of hydrogen.
[a] $SEL_{50/90\%}$ = % unsaturated amine/(% unsaturated amine + % saturated nitrile + % saturated amine) at 50/90% conversion.
[b] At maximum concentration.
[c] At maximum concentration of unsaturated amine.
[d] Selectivity to saturated nitrile (valeronitrile).
[e] Up to 30 wt.% of by-products formed.

4. Conclusions

Amorphous NiB and CoB alloys and their Cr-doped equivalents were all active catalysts in the hydrogenation of unsaturated nitriles. Their activity can be accounted to the presence of different types of bonded hydrogen and their unique electronic structure. The hydrogenation of unsaturated nitriles over NiB(Cr) catalysts proceeded via the saturated nitrile due to the high activity of nickel catalysts towards C=C bond hydrogenation caused by the presence of weakly bonded hydrogen. The hydrogenation over CoB(Cr) catalysts, which showed lower activity in C=C bond hydrogenation, but higher activity in the reduction of C≡N bond, occurred preferentially via the unsaturated amine. The electron donation from boron to cobalt reinforced the adsorption of C≡N group by increasing the backdonation into the CN anti-bonding orbital, which increased the selectivity to nitrile hydrogenation. The chromium doping suppressed the agglomeration of boride particles and increased the active surface area, which results in higher activities of Cr-doped catalysts. Moreover, it was found by TPD measurements that the Cr-doped catalysts contain a higher amount of weakly bonded hydrogen, which could be responsible for preferential C=C bond hydrogenation. The chromium species can also act as Lewis sites, which facilitate the adsorption of the nitrile group of the substrate molecule at the surface of the catalyst. The NaOH treatment of the CoBCr catalyst probably caused the removal of weakly bonded hydrogen from the surface of the catalyst, and, thus, increased the selectivity to unsaturated amine. One of the main advantages of the boride catalysts was also the suppression of by-product formation without any addition of a base. This shows that the unsaturated nitriles can be selectively hydrogenated to unsaturated amines even in the absence of ammonia.

Acknowledgements

The authors thank Professor Roel Prins for carefully reading the manuscript, Dr. Petr Sajdl for carrying out the XPS measurements, and the Grant Agency of the Czech Republic for financial support (Grant No. GAČR 104/06/0684 and 203/03/H140).

References

[1] Ullmann's Encyclopedia of Industrial Chemistry, fifth ed., vol. 2A, VCH Verlag, Weinheim, 1985, p. 1.
[2] G. Gadamasetti, M.E. Kuehe, in: A.G. Cook (Ed.), Enamines: Synthesis, Structure, and Reactions, Marcel Dekkerer, Inc., New York, 1988 , p. 531.
[3] G. Petranyi, N.S. Ryder, A. Stutz, Science 224 (1984) 1239.
[4] I. Minamida, K. Iwanaga, T. Okauchi, Takeda Chemical Industries, Ltd., US 6,407,248 (2002).
[5] Y.-S. Ho, W.-S. Lee, H. Tseng, C.-H. Chen, C.-H. Lin, P.-Y. Ho, J.-S. Chu, W.-L. Ho, R.-J. Chen, Y.-J. Wang, J.-H. Jeng, S.-Y. Lin, Y.-C. Liang, J.-K. Lin, L.-C. Chen, US Patent Application 20050032904 (2005).
[6] W. Poepel, J. Gaube, Dechema Monogr. 122 (1991) 189.
[7] B. Fell, J. Sojka, Fett Wiss. Technol. 93 (1991) 79.
[8] Fruth, J. Strauss, H. Stuehler, Hoechst AG, EP 0490382 (1992).
[9] P. Kukula, K. Koprivova, J. Catal. 234 (2005) 161.
[10] J.L. Dallons, G. Jannes, B. Delmon, Acta Chim. Hung. 119 (1985) 223.
[11] J.L. Dallons, G. Jannes, B. Delmon, Catal. Today 5 (1989) 257.
[12] G.D. Yadav, M.R. Kharkara, Appl. Catal. A: Gen. 123 (1995) 115.
[13] P. Kukula, M. Studer, H.-U. Blaser, Adv. Synth. Catal. 346 (2004) 1487.
[14] A. Baiker, Faraday Discuss. Chem. Soc. 87 (1989) 239.
[15] A. Molnar, G.V. Smith, M. Bartok, Adv. Catal. 36 (1989) 329.
[16] Y. Chen, Catal. Today 44 (1998) 3.
[17] J.-F. Deng, H. Li, W. Wang, Catal. Today 51 (1999) 113.
[18] B. Ganem, J.O. Osby, Chem. Rev. 86 (1986) 763.
[19] M. Wang, H. Li, Y. Wu, J. Zhang, Mater. Lett. 57 (2003) 2954.
[20] H. Li, H. Li, W.-L. Dai, J.-F. Deng, Appl. Catal. A: Gen. 207 (2001) 151.
[21] S. Yoshida, H. Yamashita, T. Funabiki, T. Yonezawa, J. Chem. Soc. Faraday Trans. 80 (1984) 1435.
[22] J. Fang, X. Chen, B. Liu, S. Yan, M. Qiao, H. Li, H. He, K. Fan, J. Catal. 229 (2005) 97.
[23] Y.Z. Chen, K.J. Wu, Appl. Catal. 78 (1991) 185.
[24] Y.Z. Chen, S.W. Wei, Appl. Catal. 99 (1993) 85.
[25] H. Li, X. Chen, M. Wang, Y. Xu, Appl. Catal. A: Gen. 225 (2002) 117.
[26] H. Li, H. Li, M. Wang, Appl. Catal. A: Gen. 207 (2001) 129.
[27] H. Li, Y. Wu, H. Luo, M. Wang, Y. Xu, J. Catal. 214 (2003) 15.
[28] Y. Pei, H. Hu, J. Fang, M. Qiao, W. Dai, K. Fan, H. Li, J. Mol. Catal. A: Chem. 211 (2004) 243.
[29] G.N. Glavee, K.J. Klabunde, Ch.M. Sorensen, G.C. Hadjapanayis, Langmuir 8 (1992) 771.
[30] G.N. Glavee, K.J. Klabunde, Ch.M. Sorensen, G.C. Hadjapanayis, Inorg. Chem. 32 (1993) 474.
[31] A. Corrias, G. Ennas, G. Licheri, G. Marongiu, G. Paschina, Chem. Mater. 2 (1990) 363.
[32] H. Li, Y. Wu, J. Zhang, W. Dai, M. Qiao, Appl. Catal. A: Gen. 275 (2004) 199.
[33] I. Grohmann, E. Kemnitz, A. Lippitz, W.E.S. Unger, Surf. Interface Anal. 23 (1995) 887.
[34] R. Brown, M.E. Cooper, D.A. Whan, Appl. Catal. 3 (1982) 177.
[35] S.D. Robertson, B.D. Mc Nicol, J.H. de Baas, S.C. Kloet, J. Catal. 37 (1975) 427.
[36] S.D. Yim, I.S. Nam, J. Catal. 221 (2004) 601.
[37] L.I. Llieva, D.H. Andreeva, Thermochim. Acta 265 (1995) 223.
[38] B.A. Sexton, A.E. Hughes, T.W. Turney, J. Catal. 97 (1986) 390.
[39] H.-Y. Lin, Y.-W. Chen, Mater. Chem. Phys. 85 (2004) 171.
[40] F.B. Noronha, C.A. Perez, M. Schmal, R. Fréty, PCCP 1 (1999) 2861.
[41] F. Delbecq, P. Sautet, J. Catal. 152 (1995) 217.